Numerical fatigue damage analysis of a variable speed Francis pump-turbine during start-up in generating mode

To cite this article: Daniel Biner *et al* 2022 *IOP Conf. Ser.: Earth Environ. Sci.* **1079** 012079

Numerical fatigue damage analysis of a variable speed Francis pump-turbine during start-up in generating mode

Daniel Biner[1,3,*], Sebastien Alligné[2], Christophe Nicolet[2], Drazen Dujic[3] and Cécile Münch-Alligné[1]

[1] Institute of Systems Engineering, School of Engineering, HES-SO Valais-Wallis, Rue de l'Industrie 23, Sion, Switzerland
[2] Power Vision Engineering Sàrl, St-Sulpice, Switzerland
[3] Power Electronics Laboratory – PEL, Ecole Polytechnique Fédérale de Lausanne, Lausanne, Switzerland

E-mail: daniel.biner@hevs.ch

Abstract. Variable speed hydropower units offer a large spectrum of grid regulation services and may therefore contribute to the stability of future power supply systems. Full Size Frequency Converters (FSFC) already found real world application in Pumped Storage Hydropower Plants up to a rated power of 100 MW and are even considered scalable up to a few hundred MW. Apart from the extension of the power range and grid regulation capacities, the FSFC technology also provides new control possibilities during transient operations such as start-up in generating mode. Thus, harsh conditions with damaging impact on the hydromechanical components may be avoided by tuning the operating point trajectory in the start-up phase. In this paper, runner fatigue damage during start-up in generating mode of a 5 MW variable speed Francis pump-turbine prototype equipped with a FSFC is numerically analyzed. The fixed speed solution is compared to a variable speed solution following a BEP tracking control strategy. 1D hydraulic transient simulations provide boundary conditions for detailed 3-D CFD/FEA simulations. Full and reduced numerical domains are used and compared. The overall outcome of the present numerical study indicates an important reduction of partial damages using variable speed drives for turbine start-up manoeuvres.

Keywords: Reversible Francis Pump-Turbine, Variable Speed Drive, Turbine Mode Start-Up, One-Way FSI Simulation, Fatigue Damage Analysis

1 Introduction

The expected massive integration of new Renewable Energies in future energy systems increases the need of regulation elements to ensure grid stability. Hydropower already plays a role in providing ancillary grid services due to its capability to generate or absorb hundreds of MW in terms of minutes as well as its efficient energy storage capability. However, to provide frequent grid regulation services, partial damages caused by transient operation must carefully be analyzed. Frequent start and stop cycles of conventional hydropower plants may drastically

accelerate fatigue damage of hydro-mechanical components like runners as experienced in [1]. To overcome such issues, modern technologies like variable speed drives [2], dedicated to the optimization of hydropower plants in terms of life cycle and flexibility operation, are investigated and demonstrated in the XFLEX HYDRO project [3]. A new reversible pump-turbine unit that is part of the Z'Mutt power plant forms one of the demonstrators for variable speed technologies. Potential start-up strategies of the 5 MW prototype equipped with a Full Size Frequency Converter (FSFC) have numerically been analyzed in the early project stage employing 1-D hydraulic transient [4] and 3-D CFD/FEA simulations with simplified numerical domain [5]. The preliminary study indicated importantly reduced partial runner fatigue using the FSFC to start-up the unit in generating mode. To consolidate those results and to explore further strategies, the present work deals with additional numerical analyses of flexible start-up processes. A conventional fixed speed start-up is compared to a variable speed start-up applying a BEP tracking strategy. The two operating point trajectories are first determined by 1-D hydraulic transient simulations that provide the boundary conditions for 3-D CFD computations. In contrast to fully transient simulations of the start-up sequence, as presented for example in [6], the quasi-steady hypothesis is presumed with important reduction of computational effort. Thus, sets of fixed operating points on the two trajectories are simulated. The computed unsteady pressure fields are finally used for one-way coupled FSI simulations of the runner structure to estimate the fatigue damage induced by each operating point trajectory. Reduced and full CFD/FEM models are used and compared.

2 Numerical methodology

2.1 1-D hydraulic transient simulations

A SIMSEN model of the Z'Mutt power plant, as detailed in [4], is used to simulate both hydraulic transients of a conventional and a variable speed turbine start-up of the Z'Mutt pump-turbine prototype. In case of the fixed speed technology, the unit is disconnected from the power network and its rotational speed is increased by the turbine speed regulator acting on the guide vane opening to reach the nominal rotational speed. After synchronization process, the unit is connected to the power network. In case of the variable speed technology, the unit is initially connected to the power network before the start-up sequence. A linear guide vane opening law is imposed and the rotational speed is controlled by the FSFC to get the local BEP at several discrete guide vane openings. The targeted set point is estimated to correspond to the maximum generating power of the unit, thus, maximum head conditions are imposed. In figure 1 left, the SIMSEN results of the conventional start-up are shown with a grid synchronization period of about 15 s and total duration of 34.3 s to reach 95 % of the rated power. In contrast, no synchronization phase of the electrical machine is required in the variable speed case depicted on the right, since the converter is always connected to the grid. The latter scenario takes only 12.3 s to reach 95 % of the rated power. The operating points chosen for the subsequent CFD/FEA simulations are indicated by the marker points (the rated point corresponds to the asymptotic values of the curves). See figure 5 for a better understanding for the choice of the operating points. One may notice that the head fluctuation amplitudes in the variable speed case are smaller compared to the conventional case and the nominal head is never exceeded during the transient.

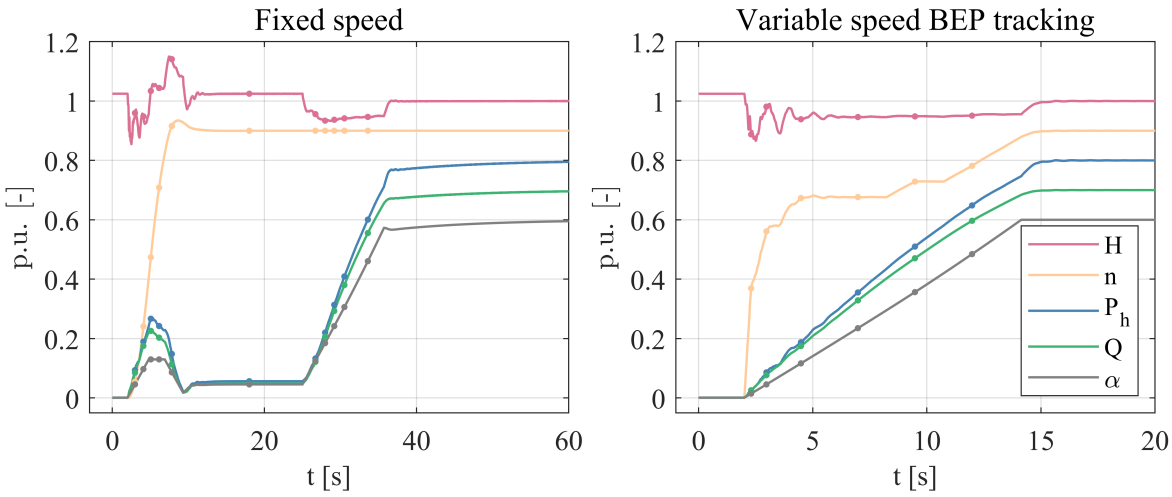

Figure 1: Pump-turbine hydraulic transients from 1-D SIMSEN simulations comparing fixed speed and variable speed start-up in turbine mode.

2.2 CFD simulations

CFD simulation techniques for hydraulic machines, as thoroughly described in [7], are widely adopted on industrial design procedures. Increasing effort is dedicated to research on off-design and transient operation indicating the need for more flexible operation and maintenance optimization of hydropower plants. Examples of flow analyses at no-load conditions experienced during conventional turbine start-up phases and often subjected to high structural damages are presented in [8] and [9]. For the present study, block structured meshes with hexahedral elements are created for all fluid domains with the software Ansys ICEM CFD R19.3. The reduced CFD domains consist of a simplified segment of the spiral casing, one stay vane passage, two guide vane passages, a single runner blade passage and the full draft tube as shown in figure 2. To handle the unequal pitches at the sliding mesh interfaces, the Profile Transform blade row model is applied for both, the steady and unsteady state simulations. This model implies temporal inaccuracy of RSI phenomena between guide vanes and runner as well as a highly approximate flow profile at the draft tube inlet. Capabilities of reduced domain CFD models for high head Francis turbines are discussed in [10]. The full meshes are presented in figure 3 and detailed information with quality metrics are given in table 1. Grid convergence in the context of fatigue damage simulations is discussed in [11] and grid size for this study is chosen accordingly.

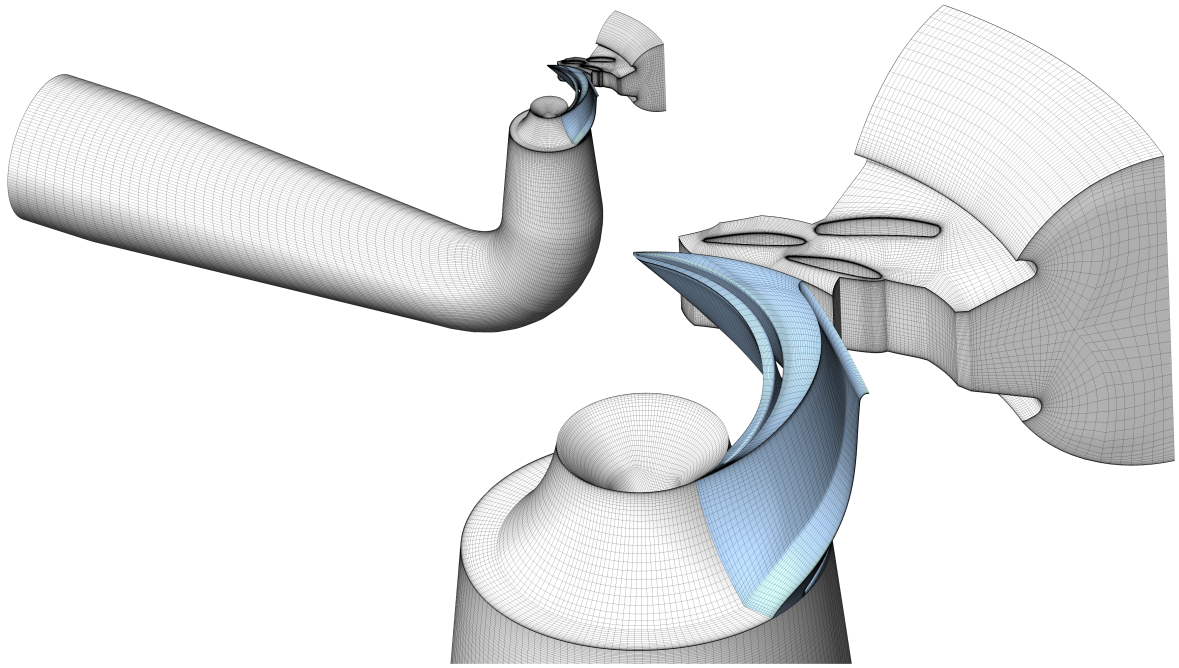

Figure 2: Partial domain CFD meshes.

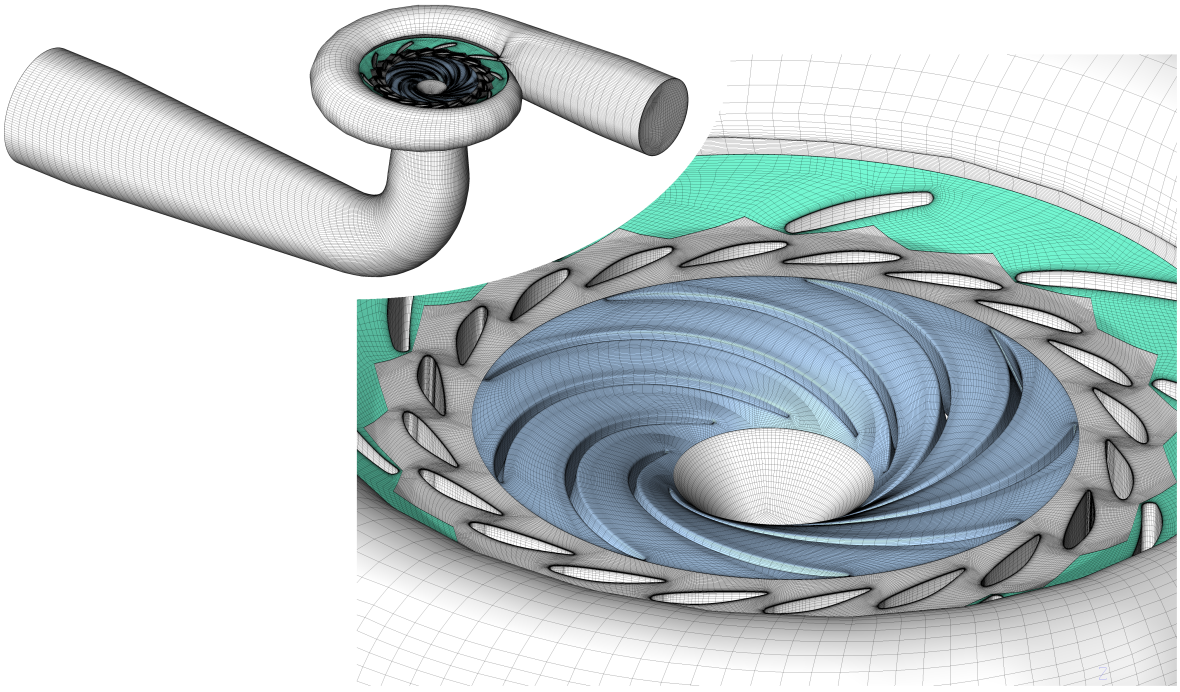

Figure 3: Full domain CFD meshes.

Table 1: Mesh size and quality.

Domain	**Number of elements** [-]	**Max. aspect ratio** [-]	**Min. face angle** [deg]	**Max. y^+** [-]	**Mean y^+** [-]
Full spiral casing	390'656	628	21.7	164.2	69.0
Full stay vanes	566'748	272	25.2	170.6	80.0
Full guide vanes	3'647'200	36.8	338.0	101.4	49.0
Full runner	2'908'764	1'565.5	27.1	132.7	38.4
Full draft tube	725'840	1290.8	36.2	114.0	26.4
Partial spiral casing, stay vanes, guide vanes	822'214	411.0	33.0	187.5	55.5
Partial runner	323'196	1'565.5	27.1	130.0	39.0
Total full domain	8'239'208				
Total partial domain	1'871'250				

The y^+ values refer to the BEP unsteady simulation at the final time step.

The flow is calculated with the CFD solver Ansysy CFX 19.3. A steady state solution with Frozen Rotor pitch change model is first computed to be imposed as initial condition to the unsteady state simulations. The SST-kω turbulence model is used with Ansys CFX's High Resolution scheme for advection terms and turbulence transport equation. Despite the URANS approach is not able to predict all aspects of the flow at no-load and low-load conditions, it is still considered reasonable to predict the most dominant pressure amplitudes that are potentially harmful to the mechanical structure. This statement may not be true in case of resonance conditions where low energy pressure amplitudes may play a role in excitation phenomena. The time step is chosen to correspond to 1.8° of rotation or to be <= 1e-3 s in case of low rotational speed values. Seven rotations are simulated for most of the operating points. The results of the three last rotations are used to determine the average hydraulic characteristics and to perform the FSI simulations. A RMS convergence level of 1e-5 is targeted that is mostly achieved within six to twelve inner iteration loops. In case of the full domain, the relative static pressure with zero gradient velocity and turbulence is imposed at the inlet boundary. In case of the partial domain, an opening condition with appropriate flow direction and 5 % turbulence intensity is defined. At the outlet boundary of both setups, the relative static pressure level is set using an opening condition with pressure driven flow direction.

2.3 One-way coupled FSI simulation

One-way coupling is chosen to investigate fatigue damage of the pump-turbine runner. This approach is considered valid for out of resonance conditions with small displacement amplitudes where hydrodynamic damping is not crucial and no vortex lock-in phenomena are expected. The structural part of the runner is discretized by quadratic tetrahedral elements counting 662'741 nodes for the full domain and 213'033 nodes for the simplified domain. The unstructured meshes are displayed in figure 4 along with the mesh refinements at the potential stress concentration and fatigue hot spots at the blade-hub and blade-shroud transitions. In case of the full domain, only one blade is refined with a mesh density similar to the reduced model. The unsteady pressure fields from CFD are mapped to the structural mesh using the implicit transient solver Ansys Workbench Mechanical R19.3, adopting the same time step as for the flow simulations. Default numerical damping is used since no resonance conditions are expected. For most operating points, three runner rotations are simulated and the temporal stress signals are extracted at the hot spot regions for fatigue calculations. Cyclic conditions are imposed at the periodic boundaries of the partial domain mesh and a fixed support is defined at the shaft connection

face. Linear pressure profiles are applied to the labyrinth gap of crown and band.

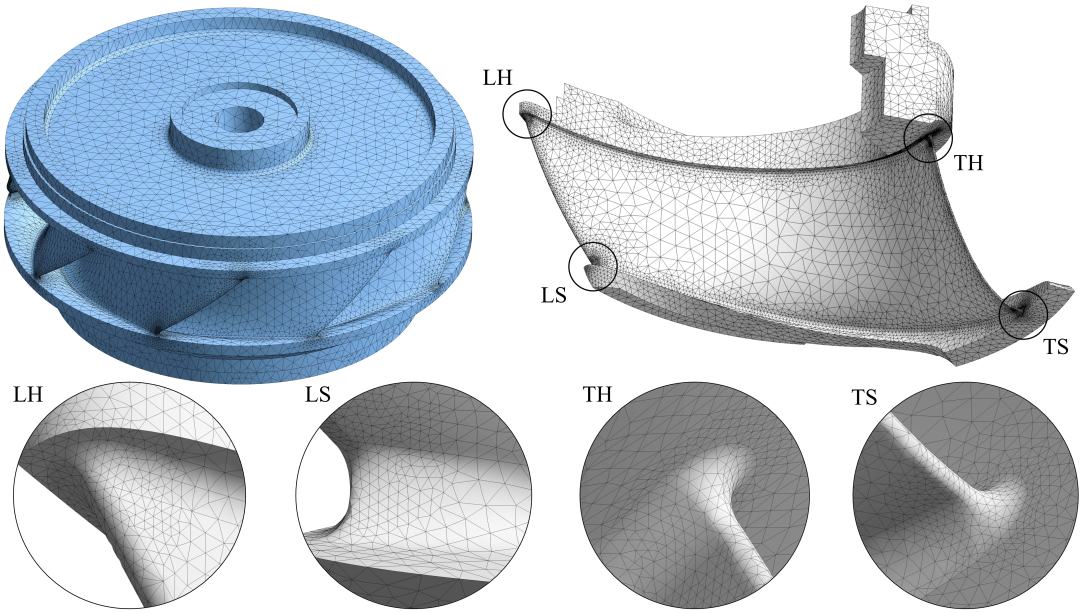

Figure 4: Full (blue) and reduced (grey) FEA meshes for one-way FSI simulations with detailed views of the potential stress concentration hot spots at leading edge - hub (LH), leading edge - shroud (LS), trailing edge - hub (TH) and trailing edge - shroud (TS) transitions.

2.4 Fatigue damage calculations

An analytical formulation based on common S-N curve properties is adopted to estimate the runner fatigue damage. The considered S-N curve yields a slope of "-1/3" in the $\log_{10}$-$\log_{10}$ S-N plane without considering any endurance limit. Thanks to standardization by a reference damage rate at BEP, the vertical intercept of the S-N curve is not required. The relative damage rate at operating point p is expressed as follows:

$$\dot{D}_p^* = \frac{t_{BEP} \sum_{i=1}^{I} D_{p,i}}{t_p \sum_{j=1}^{J} D_{BEP,j}} = \frac{t_{BEP} \sum_{i=1}^{I} n_{p,i} \Delta\sigma_{p,i}^3}{t_p \sum_{j=1}^{J} n_{BEP,j} \Delta\sigma_{BEP,j}^3} \tag{1}$$

where i or j are the indices of identified cycles, n is the cycle count, $\Delta\sigma$ is the cycle's stress range and t is the time frame of the analyzed stress signal. A linear interpolation between the points p is applied to approximate the relative damage rate function $\dot{D}^*(t)$ to finally reveal the accumulated relative damage value during the event:

$$D^* = \int_{t_0}^{t_1} \dot{D}^* dt \tag{2}$$

3 Results

3.1 Hydraulic characteristics and flow patterns

The simulated operating points expressed in the standardized $Q_{11}^*(n_{11}^*)$ hydraulic characteristics are shown in figure 5.

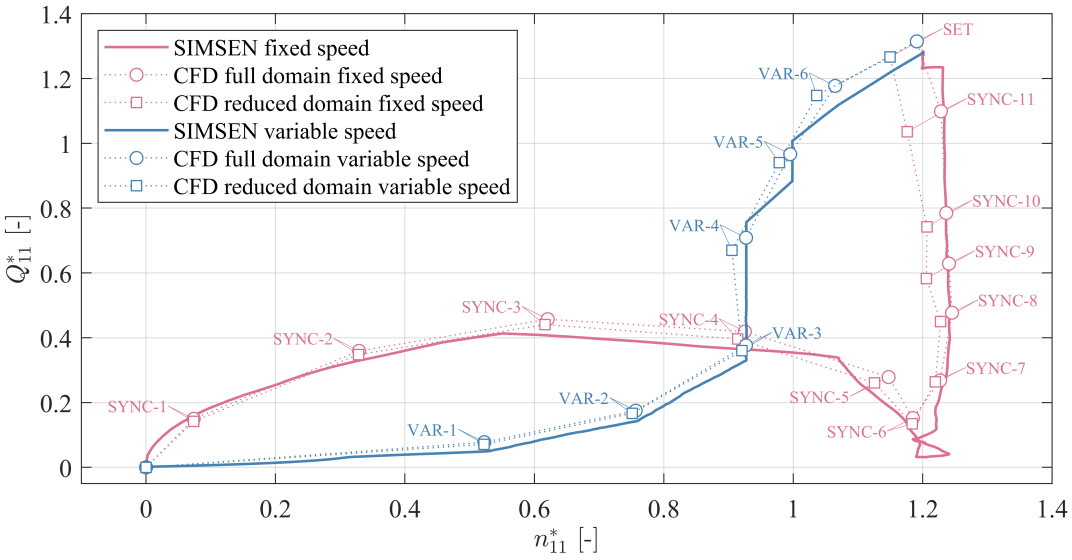

Figure 5: Trajectories of hydraulic characteristics comparing 1-D SIMSEN results to 3-D CFD result with full and reduced model.

The full domain CFD solution is generally in good agreement with the manufacturer's model test data used in SIMSEN. More important discrepancies are observed between the full and partial CFD setup. The analyses show that this difference is partially explained by the difference in the total head due to unequal dynamic pressures at the inlet boundaries of the two setups. The flow velocity is higher at the reduced domain inlet, whereas the same static pressure is imposed, thus, the total head (based on dynamic and static pressure) is increased. This effect is confirmed by the fact that the differences increase with increasing discharge or Q_{11}^* values. The static pressure at the reduced domain inlet boundary should be considered to be corrected in future analysis according to the estimated difference in dynamic pressure compared to the full domain inlet boundary. The swirling strength at different operating points, indicating the vortex structures at the mid-span section of the runner, is presented in figure 6. Graphical instancing is used to present the partial domain solution in full circumference. The first two operating points on the left reveal some striking flow asymmetries in the blade channels that are expected to create blade loading cycles. The reduced domain solution is incapable of predicting load cycles caused by asymmetric flow. Only at near BEP conditions, where the flow is expected to be symmetric, the simplified model may be capable of estimating the blade load cycles.

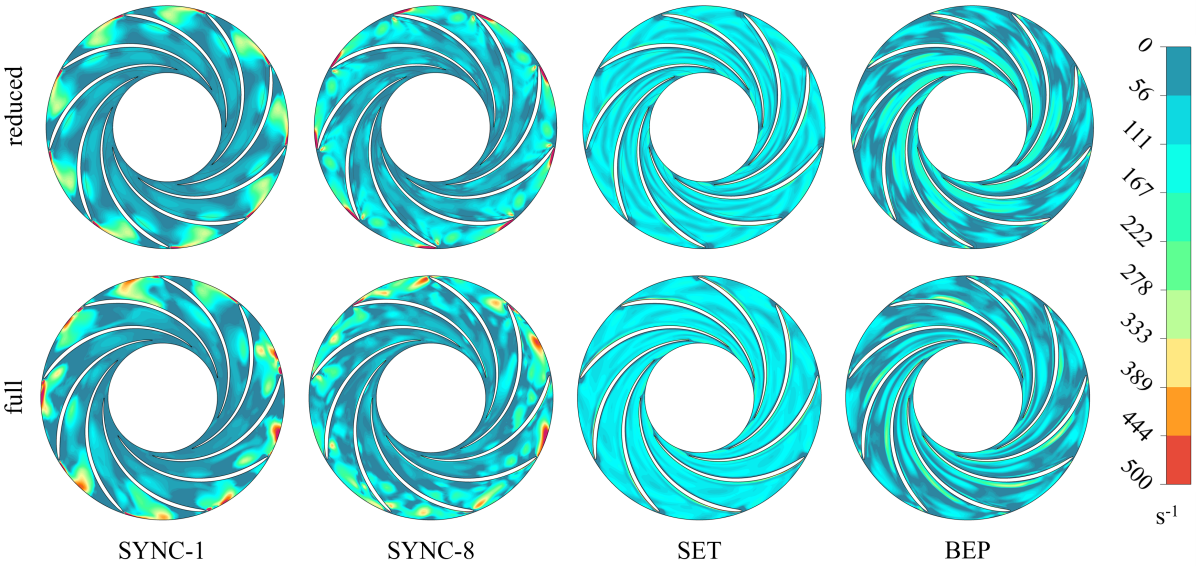

Figure 6: Instantaneous swirling strength contours at the runner mid-span section and final time step comparing reduced and full domain solutions.

3.2 Stress signals

The reference location for the results presented in this section corresponds to the mesh node that yields the maximum damage rate under BEP conditions. This reference damage hot spot is located at the leading edge-shroud (LS) transition (see figure 4). The Von Mises stress signals standardized by the average stress value at BEP of the full domain solution are presented in figure 7. Figure 7a shows the stress evolution of the fixed speed operating points including no-load (SYNC-6) and deep part load conditions (SYNC-7 to SYNC-8) with significantly increased stress level and strong stochastic fluctuations. A relatively high stress amplitude synchronized with the rotational frequency is observed at the set point, indicating an inhomogenous flow distribution in the spiral casing. The tendencies of the stress evolution are captured by the partial domain setup to some extent. However, the discrepancies in the frequency content and stress amplitudes are important and non-negligible at several operating point including the set point. Figure 7b shows the stress evolution of the variable speed start-up where the maximum stress levels are achieved at the set point and the stress signatures are mostly RSI dominated.

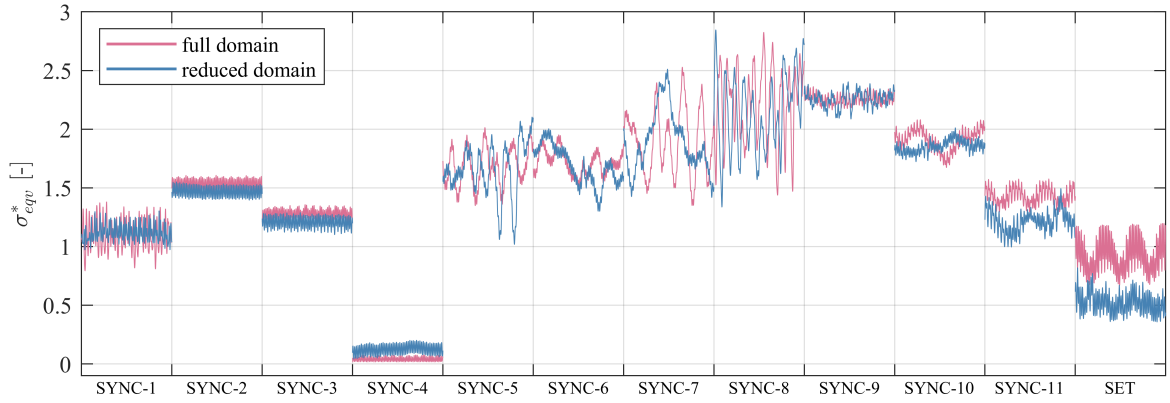

(a) Fixed speed start-up.

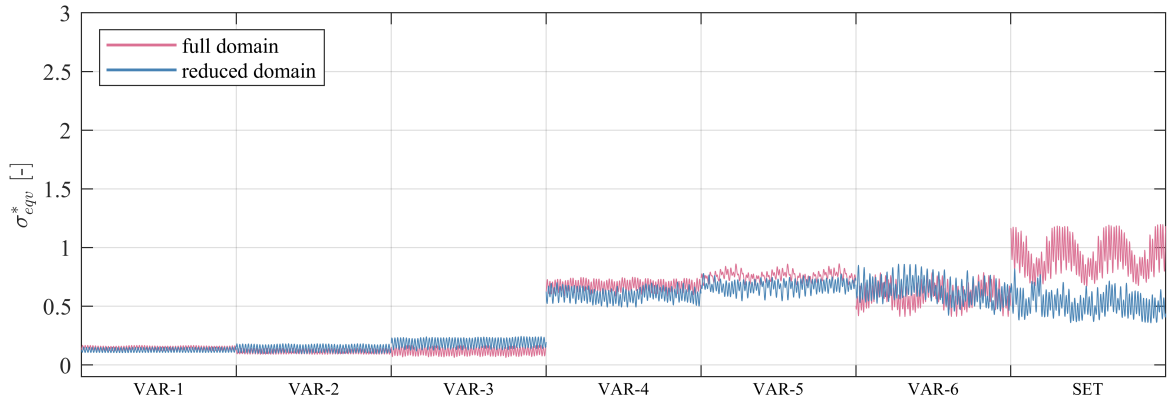

(b) Variable speed start-up.

Figure 7: Temporal evolution of standardized equivalent stress at the reference location comparing full and reduced domain solutions.

3.3 Fatigue damage results

The relative damage rate at the reference location as function of time is plotted in figure 8 left. As suspected from the stress signals, an important increase of the relative damage rate is observed in the deep part load regime with a peak value of almost 50 at operating point SYNC-8. At no-load conditions (8 s to 23 s), only slightly increased fatigue is present compared to the BEP. The maximum damage rate experienced during the variable speed start-up occurs only at the set point that lets anticipate that no significant additional fatigue cycles are induced applying the FSFC technology. In figure 8 right, the cumulative damage is displayed and reveals a total damage reduction by 7.7 times applying the variable speed BEP tracking strategy for turbine start-up. The reduced domain simulations are capable of approximating the tendencies of the damage evolution, but show non-negligible errors compared to the full simulation solutions. Part of these discrepancies may be caused by the unequal head conditions as discussed in section 3.1.

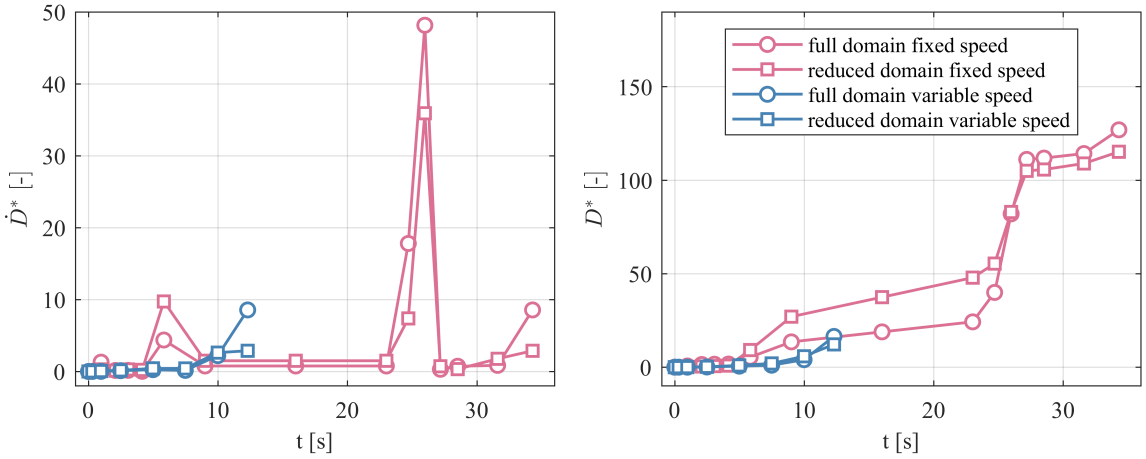

Figure 8: Relative damage rate (left) and cumulative relative damage (right) at the reference location.

3.4 Damage hill chart

For preliminary multi-objective optimization of the turbine start-up sequence, additional operating points covering a large area of the turbine operation quadrant are simulated using the full domain CFD/FEA model. Since the location of the damage hot spot is not fix, a conservative formulation is introduced for a global evaluation of the runner fatigue risk. The global relative damage rate (3) is therefore defined by the sum of the relative damage rates at the four critical blade locations illustrated in figure 4. Again, the local maximum damage rate at BEP defines the reference nodes for each of the four details.

$$\dot{D}^*_{glob} = \frac{\sum \dot{D}^*_i}{\sum \dot{D}^*_{i,BEP}}, \qquad i = [LH, LS, TH, TS] \tag{3}$$

The global relative damage hill chart with the fixed speed and variable speed BEP tracking trajectories is presented in figure 9. Moreover, the variable speed scenario with linear speed control function as investigated in [4] and [5] is indicated. It must be noticed that the damage peak at $n^*_{11} = 0.48$ and $Q^*_{11} = 0.88$ could not be detected by the reduced domain setup and therefore, the damage estimations presented in the previous studies turned out underestimated for the variable speed scenario with linear speed increase. Simplified domain simulations far from the best efficiency line are therefore considered unreliable for fatigue damage evaluation. This is increasingly the case regarding the structural dynamic response facing resonance conditions. It must be mentioned that no excitation of the runner's eigenmodes (in air) is numerically observed at the investigated operating points. Although flow patterns in different Francis turbine designs as function of n_{11} and Q_{11} are similar to some extent, the structural loads and dynamic response are strongly design and scale dependent. Moreover, operating head variations may also have substantial impact on the damage image presented in figure 9. Thus, the present work should critically be treated in the context of different runner designs. Referring to experimental fatigue damage assessments of a Francis turbine runner in extended operating range [12], some parallels can be observed in the low load operation region. The well-known increase of structural loading at low load conditions is confirmed by the present work. However, the simulations do not reveal significant loading at speed no-load. This may be explained by an insufficient amount of rotations simulated to develop an instability like rotating stall or the structural damage may be resonance tied at speed-no load and not be replicated by the limited frequency spectrum provided by URANS.

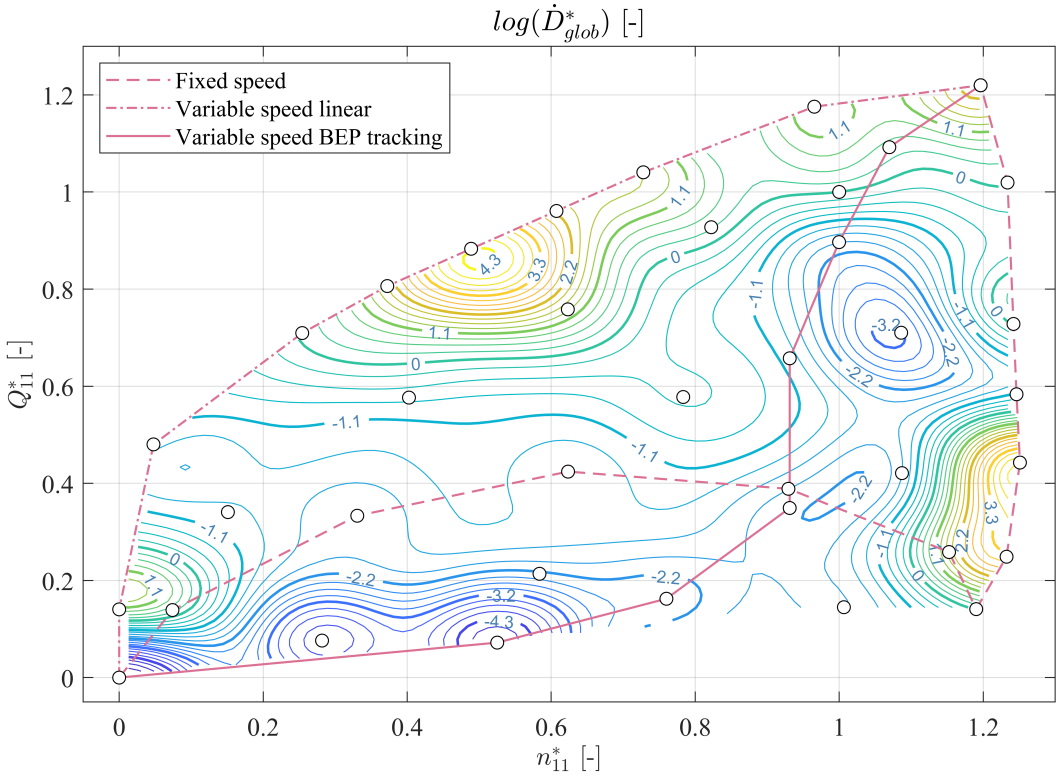

Figure 9: Simulated hill chart of global relative damage rate.

4 Conclusion

In the context of operational flexibilisation of hydropower units, the advantages of a FSFC employed for the turbine start-up of a 5 MW pump-turbine prototype are numerically investigated. In contrast to fixed speed technologies, the FSFC enables a BEP tracking strategy in the start-up phase that offers enhancements concerning runner fatigue as well as energetic losses. The CFD and FEA based numerical investigations show that the partial damage induced during the variable speed start-up sequence is reduced by a factor of about eight. Furthermore, the relative damage rate on the runner structure is characterized on a large area of the turbine operation quadrant. The deduced hill chart serves for further preliminary optimization of the speed control strategy. The simulations show that no significant additional fatigue cycles are created during the BEP tracking start-up sequence. This result lets anticipate that high frequent start and stop cycles to increase grid regulation capacities are possible without critical acceleration of runner fatigue thanks to the FSFC. Simplified numerical setups seem capable of approximating the fatigue damage tendencies to some extend but are considered unreliable for such assessments. The results presented in this paper are planned to be validated by strain measurements on the pump-turbine prototype runner to evaluate the reliability of the applied numerical approach.

Acknowledgments

The Hydropower Extending Power System Flexibility (XFLEX HYDRO) project has received funding from the European Union's Horizon 2020 research and innovation programme under grant agreement No 857832. The authors would like to thank Alpiq SA, CKD Blansko and Hydro Exploitation SA for their collaboration and support.

References

[1] Hasmatuchi V, Decaix J, Titzschkau M and Münch-Alligné C 2018 A challenging Puzzle to Extend the Runner Lifetime of a 100 MW Francis Turbine *Hydro 2018, Gdansk*
[2] Bontemps P, Hugo N and Dujic D 2020 Flexibility Enhancements in Pumped Hydro Storage PowerPlants through Variable Speed Drives *IECON 2020*
[3] Hydropower Extending Power System Flexibility (XFLEX HYDRO) `https://xflexhydro.net/` [Online.] Accessed 2022.02.01
[4] Alligné S, Béguin A, Biner D, Münch-Alligné C, Hasmatuchi V, Hugo N, Avellan F, Dujic D and Nicolet C 2021 Turbine mode start-up simulation of a FSFC variable speedpump-turbine prototype – Part I: 1D simulation *IOP Conf. Ser.: Earth Environ. Sci.* 774 012052
[5] Biner D, Alligné S, Hasmatuchi V, Nicolet C, Hugo N, Avellan F, Dujic D and Münch-Alligné C 2021 Turbine mode start-up simulation of a variablespeed Francis pump-turbine prototype – Part II: 3-D unsteady CFD and FEM *IOP Conf. Ser.: Earth Environ. Sci.* 774 012070
[6] Casartelli E, Ryan O, Schmid A and Mangani L 2019 CFD Simulation of Transient Startup for a Low Specific-Speed Pump-Turbine *IOP Conf. Ser.: Earth Environ. Sci.* 240 082007
[7] Trivedi C, Cervantes M J and Dahlhaug O G 2016 *Appl. Mech.*
[8] Decaix J, Hasmatuchi V, Titzschkau M and Münch-Alligné C 2018 *Appl. Sci.*
[9] Nennemann B, Morissette J F, Chamberland-Lauzon J, Monette C, Braun O, Melot M, Coutu A, Nicolle J and Giroux A M 2014 Challenges in Dynamic Pressure and Stress Predictions at No-Load Operation in Hydraulic Turbines *IOP Conf. Ser.: Earth Environ. Sci.* 22 032055
[10] Jakobsen K R G, Tengs E and Holst M A 2019 Reducing Computational Effort of High Head Francis Turbines *IOP Conf. Ser.: Earth Environ. Sci.* 240 072001
[11] Biner D, Bontepms P, Dujic D and Münch-Alligné C 2022 Discretization Uncertainties of Flow and Fatigue Damage Simulations of a Reversible Francis Pump-Turbine at Off-Design Operation in Turbine Mode *Advances in Hydroinformatics, "Accepted for publication"*
[12] Lowys P Y, André F, Duparchy F, Guillaume R, Ferreira J C and da Silva A F 2014 Alqueva ll and Salamonde ll: A new approach for extending turbine operation range *Hydro 2014, Como*